

## Performance of STBC Based MIMO-OFDM Using Pilot-aided Channel Estimation

Sarah Saleh Idan<sup>1,\*</sup>, Mohammed Kasim Al-Haddad<sup>2</sup>

Department of Electronic and Communications Engineering, College of Engineering, University of Baghdad, Baghdad, Iraq

[sarah.idan2006m@coeng.uobaghdad.edu.iq](mailto:sarah.idan2006m@coeng.uobaghdad.edu.iq)<sup>1</sup>, [mohammed.alhadad@coeng.uobaghdad.edu.iq](mailto:mohammed.alhadad@coeng.uobaghdad.edu.iq)<sup>2</sup>

### ABSTRACT

Many studies have been published to address the growing issues in wireless communication systems. Space-Time Block Coding (STBC) is an effective and practical MIMO-OFDM application that can address such issues. It is a powerful tool for increasing wireless performance by coding data symbols and transmitting diversity using several antennas. The most significant challenge is to recover the transmitted signal through a time-varying multipath fading channel and obtain a precise channel estimation to recover the transmitted information symbols. This work considers different pilot patterns for channel estimation and equalization in MIMO-OFDM systems. The pilot patterns fall under two general types: comb and block types, with a proper arrangement suitable to the multiple transmit antennas. The two main channel estimation methods, LS and MMSE, are compared by evaluating performance in terms of Bit Error Rate (BER) to analyze the performance of pilot-aided channel estimation for 2x2 and 4x4 MIMO arrangements utilizing LTE parameters and the effects of modifying different numbers of OFDM subcarriers under different channel models. It has been discussed, a 4x4 system performs better than a 2x2 system in terms of BER with an acceptable amount of additional complexity.

**Keywords:** MIMO-OFDM, STBC, LS, MMSE.

---

\*Corresponding author

Peer review under the responsibility of University of Baghdad.

<https://doi.org/10.31026/j.eng.2023.06.02>

This is an open access article under the CC BY 4 license (<http://creativecommons.org/licenses/by/4.0/>).

Article received: 02/10/2022

Article accepted: 20/11/2022

Article published: 01/06/2023



## أداء MIMO-OFDM بالاعتماد على STBC وبمساعدة اشارات القيادة في تقدير القناة

سارة صالح عيدان<sup>1\*</sup>، محمد قاسم محمد<sup>2</sup>

قسم هندسة الالكترونيات والاتصالات، كلية الهندسة، جامعة بغداد، بغداد، العراق

### الخلاصة

تم نشر العديد من الدراسات من أجل معالجة المشاكل المتزايدة في أنظمة الاتصالات اللاسلكية. يعد ترميز الفضاء والزمان (STBC) تطبيقاً فعالاً وعملياً من تطبيقات MIMO-OFDM وهو أداة قوية لزيادة الأداء اللاسلكي عن طريق تنوع الإرسال. باستخدام عدة هوائيات وتشفير الرموز المرسل. يتمثل التحدي الأكبر في استعادة الإشارة المرسل من خلال قناة التضاؤل الجزئي المتغيرة متعددة المسارات والحصول على تخمين دقيق لقناة الاتصال من أجل استعادة المعلومات المرسل. يأخذ هذا العمل في الاعتبار الأنماط التجريبية المختلفة لتخمين قناة الاتصال ومعادلتها. تندرج الأنماط التجريبية تحت النوعين العامين: نوع comb ونوع block بترتيب مناسب لهوائيات الإرسال المتعددة. تتم مقارنة طريقتين رئيسيتين لتخمين القناة LS و MMSE من خلال تقييم الأداء من حيث معدل الخطأ (BER) ل 2×2 و 4×4 أنظمة MIMO وأعداد مختلفة من الموجات الحاملة الفرعية لل OFDM ونماذج قنوات مختلفة.

الكلمات الرئيسية: متعدد المدخلات متعدد المخرجات-ترميز الفضاء والزمان, خطأ التريعات الأصغر, الحد الأدنى لمتوسط الخطأ التريعي.

## 1. INTRODUCTION

With the growth of wireless communication technology such as Wireless Fidelity (Wi-Fi), Long-Term Evolution (LTE), and 5G new radio (NR) to meet the users' requirements for higher data rate and better service quality, there was a need to turn to a novel technology that meets these requirements. This was the main motivation for using Multiple-Input, Multiple-Output (MIMO) merged with Orthogonal Frequency-Division Multiplexing (OFDM) for its higher spectral efficiency and robustness against fading channels without additional transmit power or increase of bandwidth. The main advantages of MIMO systems are diversity gain and multiplexing gain. Diversity gain is achieved by sending multiple copies of data symbols through multiple transmit antennas and receiving them through multiple receive antennas to reduce the channel fading effect and increase the channel reliability. Multiplexing gain is achieved by sending independent data streams through multiple transmit antennas; as a result, the channel capacity is increased (Hampton, 2014; Choi et al., 2019).

Channel estimation and equalization are necessary to recover a signal transmitted through time-varying and frequency-selective channels and obtain a precise channel estimation to recognize the information symbols. Generally, there are three types of channel estimation, pilot aided channel estimation, blind channel estimation, and semi-blind channel estimation. In pilot-aided channel estimation, the channel coefficients are estimated using the transmission of known pilot symbols embedded with the data symbols in the time-frequency



lattice (Kahlon et al., 2015). Blind channel estimation is suitable for a slowly varying channel, unlike pilot-aided channel estimation (Deepak et al., 2015), which presents a novel pilot pattern produced using an NRZ encoder for semi-blind channel estimate. The pilot's pattern is such that one antenna transmits a positive pilot symbol while the other transmits negative pilot symbols instead of the zero pilot. (Zhang et al., 2018) developed a MIMO channel estimate for a fast linear time-varying multipath channel that can produce high-accuracy channel estimation using a special pilot design to reduce intercarrier interference. (Emad et al., 2017) suggested a technique where each transmits antenna's OFDM data symbol is pre-coded using a spreading matrix and using a nulling matrix at certain subcarrier locations inserts nulls. Then, orthogonal superimposed pilots have added the frequency domain for each transmit antenna, giving a more precise channel estimate. (Thomas and Noir, 2019) estimated channel performance with superimposed pilots and null subcarriers. This technique requires an iterative calculations approach; the iterative methods consume power due to their extremely demanding computational effort. To address the frequency offset and channel uncertainty problems in (MIMO-OFDM) systems (Liang and Chang, 2010) proposed a technique for estimating channel coefficients in the presence of frequency offset using the pilot symbols technique based on the characteristics of the discrete Fourier transform (DFT) and Hadamard product.

This work aims to study the performance of different techniques of pilot-based channel estimations like LS and MMSE in MIMO channels was implemented and evaluated using Space Time Block Code (STBC) with different channel models and for various parameters and discusses the impact of increasing the number of antennas on the overall performance.

## 2. MIMO SYSTEM

### 2.1 MIMO-STBC Systems

One of the most popular applications of MIMO systems in terms of diversity gain is Space Time Block Coding (STBC), a powerful tool for increasing wireless communications performance to transmit diversity by employing several antennas. In STBC, a block of data symbols is encoded and sent through  $N_T$  transmit antennas and received by  $N_R$  receive antennas. Different STBC encoding tables were constructed to obtain the highest possible diversity order. As a result, STBC has become a commonly used method, as it is now defined in all modern wireless technologies that use MIMO applications. STBC requires the channel state information (CSI) at the receiver only, unlike other systems that require the CSI at the transmitter. In addition to the significant performance enhancement due to the diversity gain it provides (Achoura and Bouallegue, 2011).

To explore STBC, consider a  $2 \times 2$  MIMO system where a block of symbols is encoded according to **Table 1.**, and transmitted over different transmitter antennas.

A block of two consecutive symbols in time is encoded into two spatially separated blocks for each transmit antenna. Each block contains two symbols in time since the input block (in time) consists of two symbols, and the output block (in time) for each antenna also consists of two symbols; in this case, the coding rate is 1.

In general, the space-time encoded symbols are transmitted through  $N_T$  transmit antennas and received by  $N_R$  receive antennas, as shown in **Fig. 1**, where the lower indices represent the special indices and the index between the parentheses represents the time slot index. The received signal of the MIMO system can be expressed (Cho et al., 2011)



**Table 1.** A 2×2 STBC Encoder

Space (O/P) \ Time (I/P)	Antenna 1	Antenna 2
$s_1$	$s_1$	$s_2$
$s_2$	$-s_2^*$	$s_1^*$

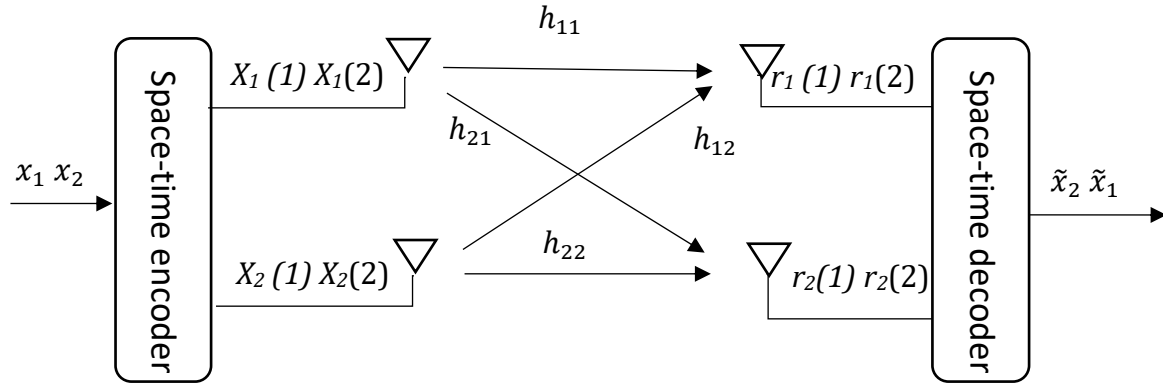


**Figure 1.** MIMO system 2×2 using STBC.

A 4×4 STBC is illustrated in **Table 2**. It is shown that a block of 3 symbols in time is encoded into four blocks for each antenna; each block contains four symbols in time, making the coding rate 3/4.

**Table 2.** A 4×4 STBC encoder with coding rate R=3/4.

Space (O/P) \ Time (I/P)	Antenna 1	Antenna 2	Antenna 3	Antenna 4
$s_1$	$s_1$	$s_2$	$s_3$	0
$s_2$	$-s_2^*$	$s_1^*$	0	$s_3$
$s_3$	$s_3^*$	0	$-s_1^*$	$s_2$
	0	$s_3^*$	$-s_2^*$	$-s_1$

The received symbols of the NR×NT MIMO system can be expressed as:

$$\begin{bmatrix} r_1 \\ r_2 \\ \vdots \\ r_i \end{bmatrix} = \sqrt{\rho} \begin{bmatrix} h_{11} & h_{12} & \dots & h_{1j} \\ h_{21} & h_{22} & \dots & h_{2j} \\ \vdots & \vdots & \ddots & \vdots \\ h_{i1} & h_{i2} & \dots & h_{ij} \end{bmatrix} \begin{bmatrix} x_1 \\ x_2 \\ \vdots \\ x_j \end{bmatrix} + \begin{bmatrix} z_1 \\ z_2 \\ \vdots \\ z_i \end{bmatrix} \tag{1}$$



where  $h_{ij}$  is the channel coefficient between the  $j^{th}$  transmit antenna and  $i^{th}$  receive antenna,  $x_j$  is the transmitted symbol at the  $j^{th}$  antenna,  $r_i$  is the received symbol at the  $i^{th}$  antenna,  $\rho$  is the signal-to-noise ratio, and  $z_i$  is the noise term at the corresponding receive antenna with unit variance. In the STBC case, the values of  $x_j$  in Eq. (1) take the values of the corresponding encoded symbols as in **Tables 1.** and **2.** The time slot index is dropped for simplicity. In vector notation

$$\mathbf{r} = \sqrt{\rho} \mathbf{H} \mathbf{x} + \mathbf{z} \quad (2)$$

where  $\mathbf{r}$  is  $N_R \times 1$  received vector,  $\mathbf{H}$  is the  $N_R \times N_T$  channel coefficient matrix,  $\mathbf{x}$  is  $N_T \times 1$  transmitted symbols vector, and  $\mathbf{z}$  is the  $N_R \times 1$  noise vector. The transmitted symbols  $[s_1 \ s_2]$  can be recovered using the following combining methods (**Hampton, 2014**) for  $2 \times 2$  Alamouti space-time coding.

$$\tilde{s}_1 = h_{11}^* r_1(1) + h_{12} r_1^*(2) + h_{21}^* r_2(1) + h_{22} r_2^*(2) \quad (3a)$$

$$\tilde{s}_2 = h_{12}^* r_1(1) - h_{11} r_1^*(2) + h_{22}^* r_2(1) - h_{21} r_2^*(2) \quad (3b)$$

By substituting the values of  $r_1$  and  $r_2$  from Eq. (1) into Eq. (3), the result can be expressed as (**Hampton, 2014**)

$$\tilde{s}_1 = \left( \sum_{i=1}^2 \sum_{j=1}^2 |h_{ij}|^2 \right) s_1 + h_{11}^* z_1(1) + h_{12} z_1^*(2) + h_{21}^* z_2(1) + h_{22} z_2^*(2) \quad (4a)$$

$$\tilde{s}_2 = \left( \sum_{i=1}^2 \sum_{j=1}^2 |h_{ij}|^2 \right) s_2 - h_{11}^* z_1^*(2) + h_{12} z_1^*(1) - h_{21}^* z_2^*(2) + h_{22} z_2^*(1) \quad (4b)$$

In Eq. (4), the signal part is multiplied by the Frobenius norm of the channel matrix, which is the sum of magnitudes squared of the channel matrix elements; this makes it more dominant than the noise term. For the  $4 \times 4$  STBC given in **Table 2.**,  $[s_1 \ s_2 \ s_3]$  can be recovered according to the following combining methods.

$$\tilde{s}_1 = \sum_{i=1}^4 h_{i1}^* r_i(1) + h_{i2} r_i^*(2) - h_{i3} r_i^*(3) - h_{i4} r_i(4) \quad (5a)$$

$$\tilde{s}_2 = \sum_{i=1}^4 h_{i2}^* r_i(1) - h_{i1} r_i^*(2) + h_{i4} r_i(3) - h_{i3} r_i^*(4) \quad (5b)$$

$$\tilde{s}_3 = \sum_{i=1}^4 h_{i3}^* r_i(1) + h_{i4} r_i(2) + h_{i1} r_i^*(3) + h_{i2} r_i^*(4) \quad (5c)$$

Eq. (5) can be expanded similarly to Eq. (3) to separate the signal from the noise term.

## 2.2 OFDM Systems

OFDM systems are commonly used to overcome the multipath effect of the channel where the transmission bandwidth is divided into  $N$  orthogonal subchannels equally spaced in frequency and divided the transmitted symbols into  $N$  streams of symbols to be transmitted as different orthogonal subcarriers. This is equivalent to taking the IDFT of the modulated symbols (**AL-Haddad, 2014; AL-Haddad, 2014; Guerra et al., 2018; Guerra et al., 2018**).

This will make the channel effect on each subcarrier a flat fading instead of frequency selective fading. Hence the channel effect on each subcarrier can be described in Eq. (1) with an additional index added as the subcarrier index. The cyclic prefix is inserted as repeated  $N_{CP}$  samples to reduce inter-symbol interference (ISI) due to multipath fading; the cyclic prefix part is not shown in **Fig. 2** for simplicity. **(Cho et al., 2011)**. The cyclic prefix is discarded at the receiver, and the remaining  $N$  samples are subjected to  $N$ -point DFT. The combining rules in Eq. (3) or Eq. (4) are applied to each subcarrier individually to decode the transmitted symbols.

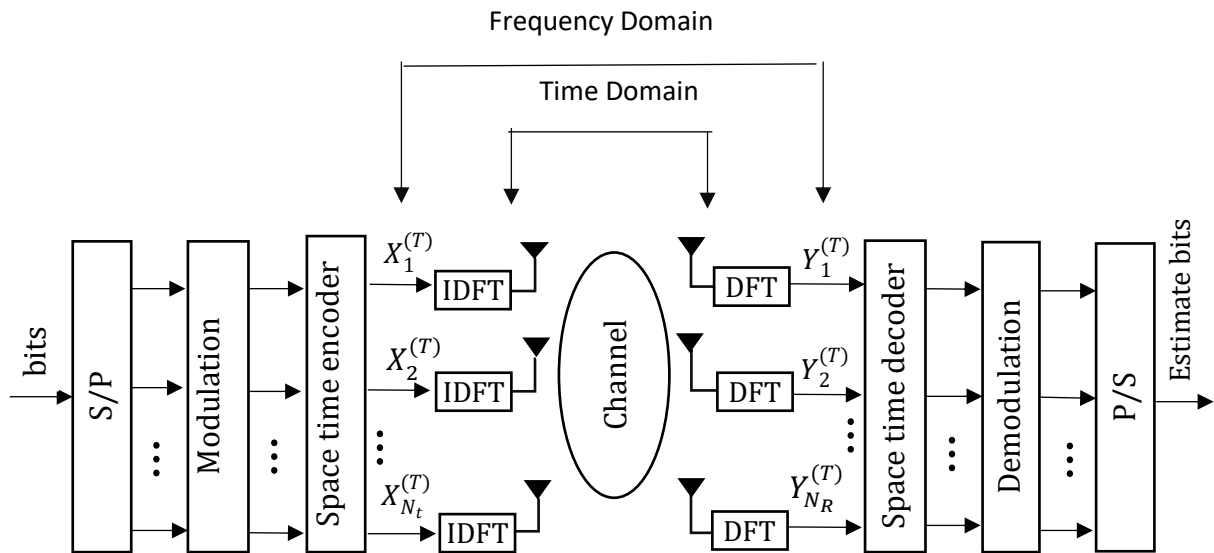


**Figure 2.** MIMO OFDM using space-time coding.

### 3. PILOT-BASED CHANNEL ESTIMATION

Channel effect needs to be estimated aiming to recover the transmitted signals; this can be obtained using known training symbols called pilots or reference signals **(Liang and Chang, 2010; Abdulmajeed and Omran, 2020)** which are known to the receiver. An important element of a MIMO-OFDM communication system design is the location of training symbols in time, space, and frequency. Two main types of pilot patterns are commonly used: comb type and block type. For a single antenna comb type, pilot symbols can be transmitted using continuous time slots for certain frequency subcarriers, as seen by the rows in **Fig. 3A**. This pilot structure is suitable for fast-varying channels, and interpolation is required in the frequency domain. In block type pattern where the pilots are sent for all subcarriers over certain time slots, as shown in **Fig. 3B (Kahlon et al., 2015)**

For **Fig. 3A**, the sequence of  $p$  pilot symbols is repeatedly transmitted in time by each of the transmit antennas. Each transmit antenna has a different pilot time pattern repeated in each pilot subcarrier. A common pilot pattern is to transmit a pilot signal for a certain transmit antenna while the remaining antennas remain silent, i.e., no signal is transmitted by the

remaining antennas, as shown in **Fig. 4**, each row represents the same pilot subcarrier for different transmit antennas.

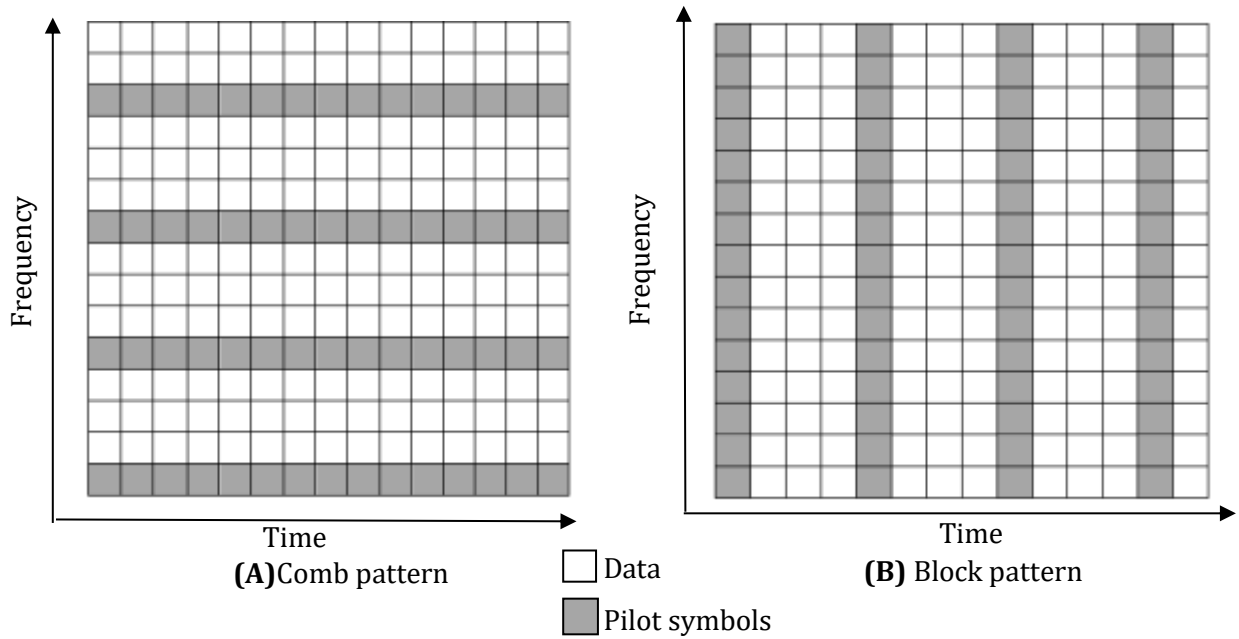


**Figure 3.** Comb and Block pilot patterns.

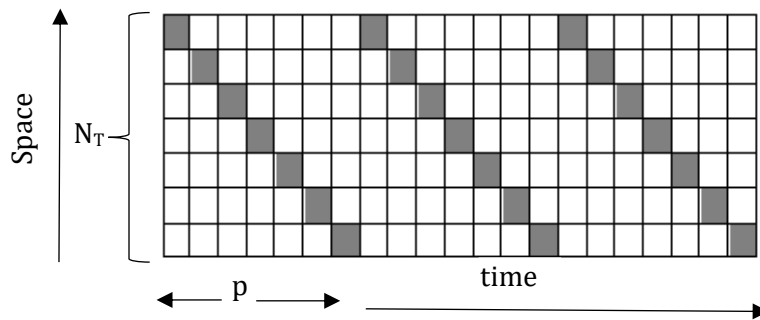


**Figure 4.** Pilot symbols allocations through  $N_T$  transmit antenna

The pilot signals in **Fig. 4** form a pattern of repeated blocks of  $N_T \times p$  symbols that can be described as an  $N_T \times p$  matrix  $S_p$ . The matrix  $S_p$  should satisfy the following two conditions (**Hampton, 2014**):

$$1- p \geq N_T \tag{6}$$

$$2- S_p S_p^H = \frac{p}{N_T} I_{N_T} \tag{7}$$

where  $A^H$  is the Hermitian transpose of the matrix  $A$ . It is a common practice to choose  $p = N_T$  resulting in a  $p \times p$  matrix and the pattern in **Fig. 4** becomes an  $I_p$  identity matrix. The different



patterns of  $S_p$ : can be the Identity, DFT, and Hadamard matrices to estimate the channel coefficient. The pattern in **Fig. 4** represents the case where  $S_p$  is  $p \times p$  identity matrix  $I_p$ , for the case of the Hadamard and complex pilot pattern  $S_p$ ,  $p=4$  is given by

$$S_p^{ID} = \frac{1}{\sqrt{N_T}} \begin{pmatrix} 2 & 0 & 0 & 0 \\ 0 & 2 & 0 & 0 \\ 0 & 0 & 2 & 0 \\ 0 & 0 & 0 & 2 \end{pmatrix} \quad (8)$$

$$S_p^{HAD} = \frac{1}{\sqrt{N_T}} \begin{pmatrix} 1 & 1 & 1 & 1 \\ 1 & -1 & 1 & -1 \\ 1 & 1 & -1 & -1 \\ 1 & -1 & -1 & 1 \end{pmatrix} \quad (9)$$

$$S_p^{DFT} = \frac{1}{\sqrt{N_T}} \begin{pmatrix} 1 & 1 & 1 & 1 \\ 1 & j & -1 & -j \\ 1 & -1 & 1 & -1 \\ 1 & -j & -1 & j \end{pmatrix} \quad (10)$$

The Identity Matrix *ID*, Hadamard *HAD*, and Discrete Fourier Transform *DFT* are better in practice than the Identity pilot matrix because the identity pattern has higher entry values that require a wider dynamic range for the same average power.

### 3.1 Channel Estimation Approaches

To investigate the performance of pilot-aided channel estimation, the following approaches can be employed:

#### 3.1.1 Maximum Likelihood (ML)

Maximum likelihood maximizes the likelihood of the function  $p(R_p|H)$  and can be described as **(Hampton, 2014)**:

$$\hat{H}_{ML} \triangleq \arg \max_{\{H\}} p(R_p|H) \quad (11)$$

where  $R_p$  is the  $N_r \times p$  matrix constructed from the received vector  $\mathbf{r}$  using  $p$  time slots corresponding to the  $S_p$  matrix of the transmitted pilots.

#### 3.1.2 Least Squares (LS)

Least Squares reduce the error between the actual values and the estimated values and can be described as **(Hampton, 2014)**:

$$\hat{H}_{LS} \triangleq \arg \min_{\{\hat{H}\}} \|\hat{R}_p - R_p\|_F^2 \quad (12)$$

Both ML and LS equations reduce to as below



$$\hat{H}_{LS} = \frac{1}{\sqrt{\rho}} (R_p S_p^H) (S_p S_p^H)^{-1} \quad (13)$$

Channel estimations using maximum likelihood and least squares have similar implementations.

### 3.1.3 Linear Minimum Mean Square Error (LMMSE).

Linear minimum mean square error minimizes the mean square error between the actual channel and channel estimation and can be described as:

$$\hat{H}_{MMSE} \triangleq \arg \min_{\{\hat{H}\}} \mathbb{E}\{\|H - \hat{H}\|_F^2\} \quad (14)$$

For the linear *MMSE* (LMMSE) case, the estimate of  $H$  can be written as

$$\hat{H} = R_p W \quad (15)$$

where  $\hat{H}$  is a linear combination of the received signal, and  $W$  is a weighting coefficients matrix, Eq. (15) is equivalent to having the error between the estimated channel coefficients and the actual channel coefficient orthogonal to the received signal  $R_p$  (**Scharf, 1991**).

$$\mathbb{E}[R_p^H E] = \mathbb{E}[R_p^H (H - \hat{H})] = \mathbb{E}[R_p^H (H - R_p W)] = 0 \quad (16)$$

And Eq. (16) can be solved for  $W$

$$W = \sqrt{\rho} (N_r I_{N_r} + \rho S_p^H R_{HH} S_p)^{-1} S_p^H R_{HH} \quad (17)$$

From Eq. (15), the *MMSE* channel estimation channel coefficients can be written as

$$\hat{H}_{MMSE} = \sqrt{\rho} R_p (N_r I_{N_r} + \rho S_p^H R_{HH} S_p)^{-1} S_p^H R_{HH} \quad (18)$$

where  $R_{HH}$  is the channel correlation matrix, and it reduces to an identity matrix  $I_p$  if the channel paths are uncorrelated (**Hampton, 2014**) and Eq. (18) is reduced to

$$\hat{H}_{MMSE} = \sqrt{\rho} R_p (I_p + \rho S_p^H S_p)^{-1} S_p^H \quad (19)$$

the values of the estimate  $\hat{H}$  from Eq. (13) or Eq. (18) are used in the combining equations given by Eq. (3) and Eq. (5).

It's important to mention that the MMSE approach has a higher level of computational complexity than the LS approach due to the complexity of the matrix inversion in Eq. (18), while in LS, the result of matrix inversion in Eq. (13) is the inversion of Eq. (7) which is quite straight forward.



#### 4. RESULTS AND DISCUSSION

The simulation results in this paper are based on the system parameters of MIMO-OFDM that are given in **Table 3**.

**Table 3.** System Parameters

Parameter	Value	
$N_T \times N_R$	2x2, 4x4	
Channel model	EPA	EVA
N: OFDM Subcarriers	128, 1024	
Cyclic Prefix Length	9, 72	
F: subcarrier frequency separation	15 kHz	7.5 kHz
$F_D$ : Maximum Doppler frequency	10Hz, 50Hz	
Modulation Technique	16-QAM	

The two MIMO configurations, 2x2 and 4x4, are investigated under two Rayleigh fading frequency selective channel models: the EPA and EVA channels models, which have a delay spread of 43ns and 356ns, respectively (**TS, 2017**). The subcarrier separation for the EPA channel is 15kHz, and the EVA is 7.5 kHz because it is more frequency selective due to its higher delay spread and hence has less coherence bandwidth. (**Jain, 2007**). The spectral efficiency in bit/sec/Hz is given by (**Hampton, 2014**)

$$\eta = \log_2 M \times R \times \frac{N}{N+N_{CP}} \times Q_p \times 100\% \quad (20)$$

where  $M$  is the constellation order and  $Q_p = (N - N_p) / N$  for comb type,  $Q_p = (N_b - p) / N_b$  for block type, where  $N$  is the number of OFDM subcarriers,  $N_p$  is the number of pilot subcarriers, and  $N_b$  is the number of OFDM symbols per block. The values of  $N_p$  and  $N_b$  are chosen such that  $Q_p = 0.9$ . The spectral efficiency according to the parameters mentioned above is  $\eta = 3.25$  for the 2x2 case and 2.24 for the 4x4 case. The pilot insertion is necessary for the channel estimation imposed about a 10% reduction in the spectral efficiency, which is quite acceptable.

**Figs. 5 to 7** show the BER performance for the LS and MMSE estimators under different parameters. MMSE estimator is slightly better than LS for the 2x2 and 4x4 MIMO systems and comb block pilot patterns. However, it is noteworthy that the complexity of the linear MMSE estimator is much higher than LS. Both estimation approaches have improved BER performance as the number of antennas increased, with approximately SNR 6dB improvement for the 4x4 over the 2x2 at  $10^{-4}$  BER.

Additionally, the BER for the comb type is about 1-2dB SNR better than the block type. The difference in performance in terms of the number of subcarriers  $N=128$  and 1024 is about 1 dB which is why the other values of subcarriers are not shown in the figures. The simulation results also show that channel parameters do not affect both pilot schemes. In particular, the comparison between **Figs. 5 and 6** shows that the performance is not affected when the channel is changed from EPA to EVA, which has a higher delay spread, leading to higher frequency selectivity and less coherence bandwidth.

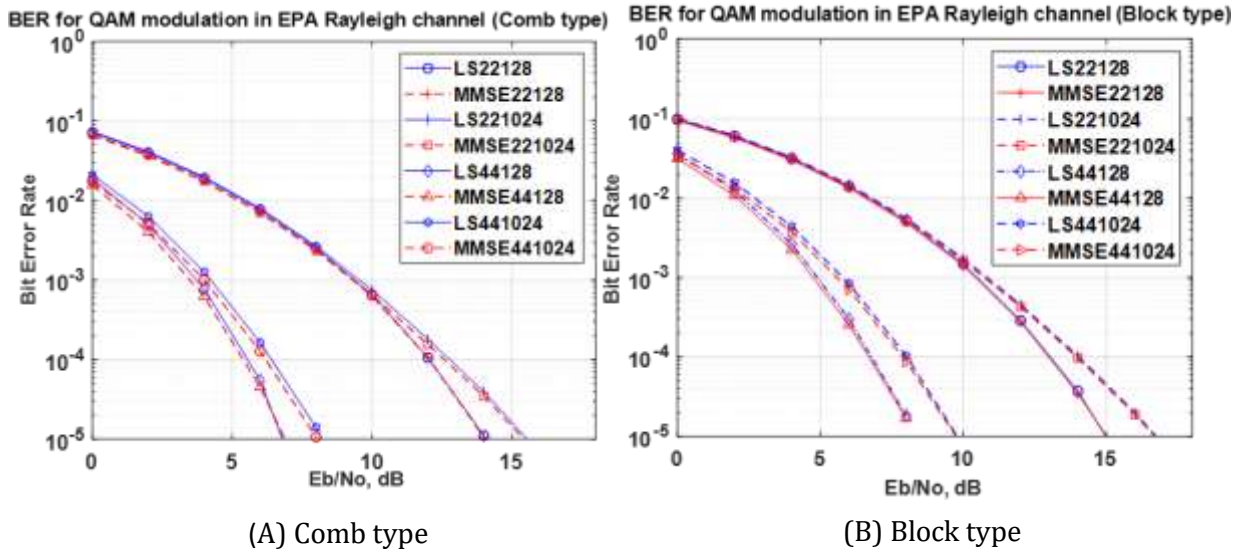


Figure 5. BER performance of LS and MMSE estimators in EPA channel for  $(2 \times 2)$  and  $(4 \times 4)$  systems with  $f_D=10$  Hz

Also, the comparison between **Figs. 5 and 7** shows that the performance is not affected when increasing the Doppler spread, increasing the channel's time variation, and reducing the channel's coherence time.

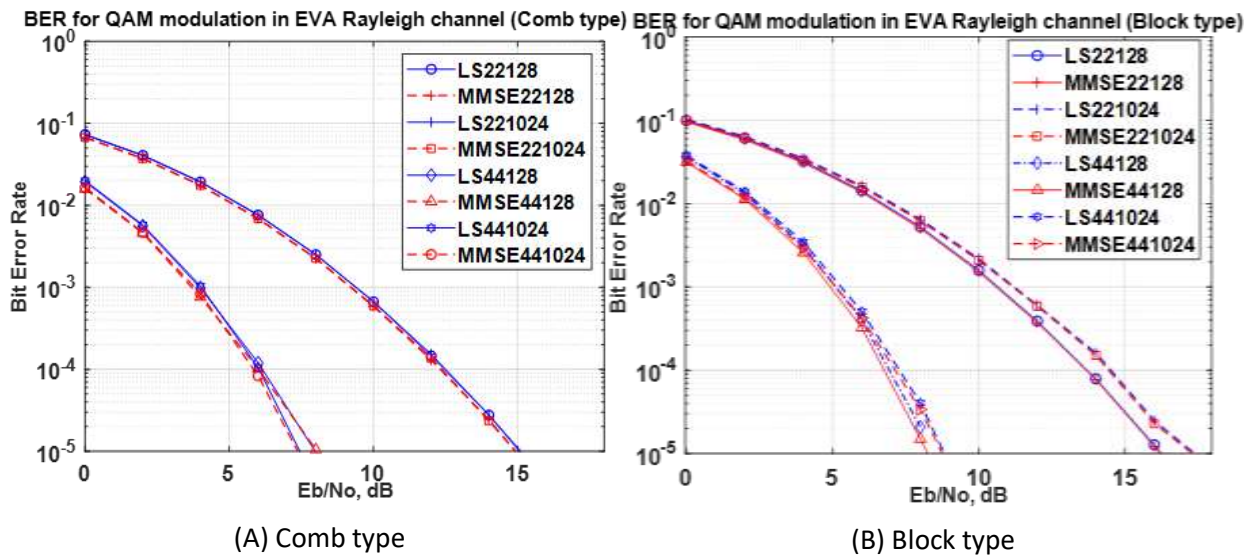
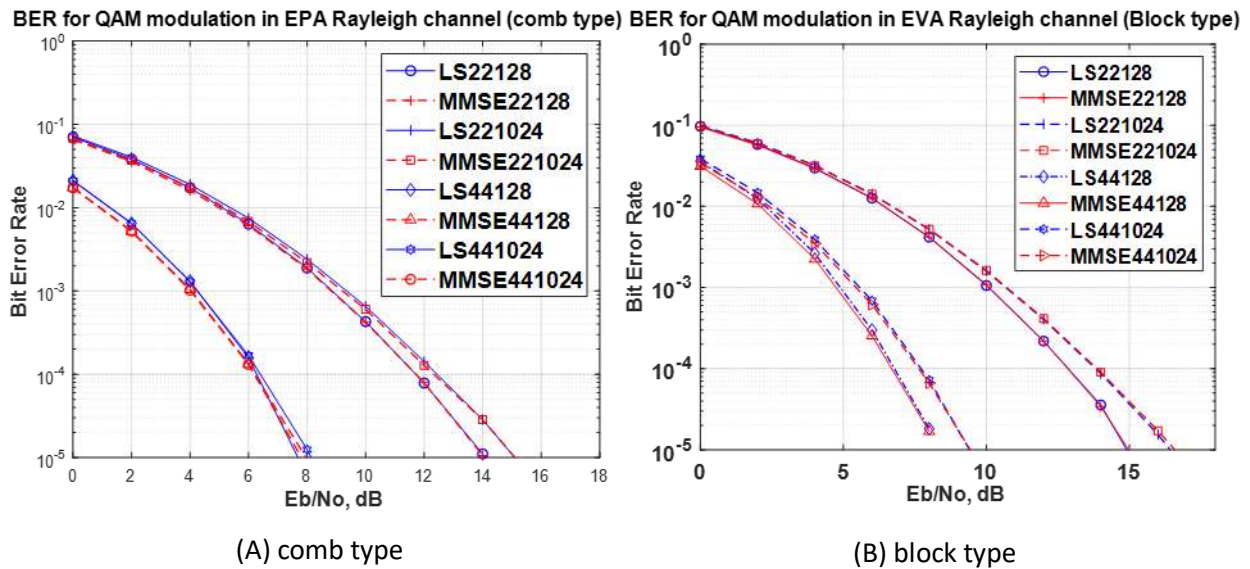


Figure 6 BER performance of LS and MMSE estimators in EVA channel for  $(2 \times 2)$  and  $(4 \times 4)$  systems with  $f_D=10$  Hz



**Figure. 7** BER performance of LS and MMSE estimators in EPA channel for (2×2) and (4×4) systems with  $f_D = 50$  Hz

### 3. CONCLUSIONS

A brief performance evaluation of MIMO-OFDM, STBC with pilot-based channel estimation has been presented. LS and MMSE channel estimation approaches have been discussed for analyzing pilot-aided channel estimation performance using LTE parameters and channel models. As the presence of inserted pilots causes spectral efficiency loss, it was necessary to establish a balance between the performance and the spectral efficiency. The simulation results show that MMSE has marginal performance improvement over LS, making its computational complexity practically unjustifiable. By altering all System Parameters, it has been observed that the BER performance of 4×4 outperforms 2×2 by 6 dB SNR, which is reasonable for the complexity difference between the two configurations. On the other hand, changing the number of subcarriers and channel type was insignificant to the overall performance making the suggested pilot schemes a preferable candidate for MIMO-OFDM channel estimation.

### REFERENCES

- Abdulmajeed, M.M., and Omran, B.M., 2020. Pilot-based channel estimation and synchronization in OFDM system. *Journal of Engineering*, 26(6), pp. 50-59, [doi:10.31026/j.eng.2020.06.04](https://doi.org/10.31026/j.eng.2020.06.04)
- Achoura, N., and Bouallegue, R., 2011. Impact of limited feedback on MIMO-OFDM systems using Joint beamforming. *IJWMN*, 3(2), pp. 39-45. [doi:10.48550/arXiv.1105.0362](https://doi.org/10.48550/arXiv.1105.0362)
- AL-Haddad, M., K., 2014. PAPR reduction of OFDM signals using clipping and coding. *Journal of Engineering*, 20(8), pp. 18-34.



Cho, Y.S., Kim, J., Yang, W.Y., and Kang, C.G., 2011. *MIMO-OFDM wireless communications with MATLAB*. Singapore; Hoboken, Nj: IEEE Press. doi:10.1002/9780470825631

Choi, S.J., Shim, S.J., You, Y.H., Cha, J., and Song, H.K., 2019. Novel MIMO detection with improved complexity for Near-ML detection in MIMO-OFDM systems. *IEEE Access*, 7, pp. 60389–60398, doi:10.1109/ACCESS.2019.2914707

Deepak, K. Malarkodi, B., and Sagar, K., 2015. NRZ encoded pilots for Semi Blind Channel estimation, *2nd International Conference on Electronics and Communication Systems (ICECS)*, pp. 360-363, doi:10.1109/ECS.2015.7124924

Emad, F., Michael, I., Mona. Z. S., and Salwa E., 2017. Channel estimation for MIMO-OFDM systems based on data nulling superimposed pilots. *Proceeding of the 21st conference of fruct association*, pp. 114-119, doi:10.23919/FRUCT.2017.8250172.

Guerra, D. W., Fukuda, R. M., Kobayashi, R. T., and Abrão, T., 2018. Efficient detectors for MIMO-OFDM systems under spatial correlation antenna arrays. *ETRI Journal*, pp. 570–581, doi:10.4218/etrij.2018-0005.

Hampton, J. R., 2014. *Introduction to MIMO communications*. Cambridge, United Kingdom: Cambridge University Press. doi:10.1017/CBO9781107337527.

Jain, R., 2007. Channel models: A tutorial, *WiMAX Forum AATG*.

Kahlon, R. K., Walia, G. S., and Sheetal, A., 2015. Channel estimation techniques in MIMO-OFDM systems – review article. *International Journal of Advanced Research in Computer and Communication Engineering*, 4(5). doi:10.17148/IJARCC.2015.45135.

Liang, Y.J., and Chang, J.F., 2010. Noniterative Joint Frequency Offset and Channel Estimation for MIMO OFDM Systems Using Cascaded Orthogonal Pilots, *IEEE Trans Veh Technol*, 59(8), pp. 4151–4156. doi:10.1109/TVT.2010.2052641

Scharf, L.L., 1991. *Statistical signal processing detection, estimation, and time series analysis*. University of Colorado at Boulder.

Thomas, A., and Nair, A.K., 2019. Null-subcarrier based channel estimation and mutual interference reduction in MIMO OFDM systems. in *Proc. Int. Conf. Wireless Commun. Signal Process. Netw. (WiSPNET)*, Chennai, India, pp. 275\_278. doi:10.1109/WiSPNET45539.2019.9032793

Zhang, L., Xiong, H., and Dai, X., 2018. A new channel estimation algorithm for fast linear-time-varying channel in MIMO-OFDM System. *IEEE 18th International Conference on Communication Technology (ICCT)*, Chongqing. doi:10.1109/ICCT.2018.8600116.

3GPP TS 36.104 version 14.3.0 Release 14, LTE; Base Station (BS) radio transmission and reception. TS, 2017.